

A Point-of-Care Device for Theophylline Quantification in Human Milk Using Laser-Induced Graphene Electrodes

Abdulrahman Al-Shami,[†] Mona A Mohamed,[†] Haozheng Ma,[†] Sina Khazaee Nejad,[†] Ali Soleimani,[†] Farbod Amirghasemi,[†] Melissa Banks,[†] Diego Garcia,[†] Alessandro Tasso,[†] Aiman A. Yaseen,[‡] and Maral Mousavi^{*,†,¶,§,||}

[†]*Alfred E. Mann Department of Biomedical Engineering, University of Southern California, 1042 Downey Way, Los Angeles, 90089, CA, USA*

[‡]*Binghamton University, School of Pharmacy and Pharmaceutical Sciences, Binghamton, NY, USA*

[¶]*Department of Chemistry, University of Southern California, 3620 McClintock Ave, Los Angeles, 90089, CA, USA*

[§]*Department of Pharmacology and Pharmaceutical Sciences, Alfred E. Mann School of Pharmacy and Pharmaceutical Sciences, University of Southern California, 1985 Zonal Avenue, Los Angeles, 90089-9121, CA, USA*

^{||}*Department of Psychiatry and the Behavioral Sciences, Keck School of Medicine, University of Southern California, 1975 Zonal Avenue, Los Angeles, 90033, CA, USA*

E-mail: mousavi.maral@usc.edu

Keywords *Theophylline, Point-of-Care, Human Breast Milk, Laser-Induced-Graphene, Drug Detection, Therapeutic Window, Milk to Plasma Ratio*

Abstract

Theophylline is a widely prescribed medication for managing asthma and chronic obstructive pulmonary disease (COPD). This medication has a narrow therapeutic range (55–110 μM in blood), where subtherapeutic levels reduce efficacy. Excessive doses can lead to severe side effects, including nausea, arrhythmias, seizures, bradycardia, hypotension, fainting, and, in extreme cases, heart attack or death. Additionally, theophylline has a high transfer ratio (70%) from blood to breast milk, posing potential risks to breastfed infants. Monitoring theophylline concentrations in human milk can provide an estimate of maternal serum levels while ensuring the safety of breastfeeding. Despite this clinical necessity, no point-of-care (PoC) devices currently exist for at-home monitoring of theophylline levels in breast milk. To address this gap, we developed an electrochemical PoC device for theophylline quantification in human milk without requiring additional sample processing. The sensor was fabricated using laser-induced graphene (LIG) electrodes without surface modification and covered with an absorptive fiberglass layer. We show that the sensor can quantify theophylline in milk directly without any sample processing in less than one minute. A sensitivity of 0.03 $\mu\text{A}/\mu\text{M}$ and a limit of detection (LOD) of 6.5 μM were achieved, both of which are appropriate for monitoring therapeutic theophylline levels in human milk. Selectivity is demonstrated against naturally occurring compositional variations in human milk across different lactation stages and against potential electroactive drugs that may also be transferred into breast milk. The sensor provided accurate measurements in spiked human milk samples collected at the 1st, 6th, and 12th months postpartum, with recovery values ranging between 99.2% and 111.0%. This innovative PoC device represents a significant advancement in maternal and infant healthcare by allowing mothers taking theophylline to monitor their dosage effectively while preventing potential neonatal exposure through breastfeeding.

Introduction

Theophylline, also known as 1,3-dimethylxanthine, is an alkaloid found in various plants such as cocoa beans and tea leaves.^{1,2} Theophylline is a commonly prescribed medication for managing asthma and chronic obstructive pulmonary disease (COPD) around the world.^{3,4} Theophylline restores levels of HDAC2 (histone deacetylase 2) by selectively inhibiting PI3K δ (phosphoinositide 3-kinase delta), an enzyme that becomes active due to oxidative stress in patients with chronic obstructive pulmonary disease (COPD).^{5,6}

Theophylline's optimal therapeutic effects occur within a narrow plasma concentration range of 55–110 μM .^{1,7–9} Below 55 μM , the drug's effects are clinically insignificant, while concentrations above 110 μM result in adverse side effects, such as nausea, arrhythmias, seizures, slow heart rate, weak pulse, fainting, and in severe cases, heart attack or even death.^{7,10,11} Therefore, it is highly recommended to monitor theophylline levels in the body to ensure accurate dosing that avoids toxicity while maintaining efficacy. Moreover, the concentration of theophylline also depends on factors that affect its clearance, such as P450 (CYP1A2) inducers (e.g., rifampicin, smoking), a high-protein diet, P450 inhibitors (e.g., cimetidine), liver disease, viral infections, and aging, highlighting the need for individualized monitoring.^{12–14}

Various laboratory-based analytical techniques have been employed for theophylline quantification, such as high-performance liquid chromatography (HPLC),¹⁵ capillary electrophoresis,¹⁶ fluorescence polarization immunoassay,¹⁷ radioimmunoassay,¹⁸ and capillary chromatography.¹⁹ However, those techniques often demand specialized expertise, and high costs. and extensive sample preparation, and processing times.^{9,20} Electrochemical methods effectively address the limitations of traditional analytical techniques by offering advantages such as speed, precision, portability, and affordability.^{9,21–26} For instance, electrochemical biosensors were designed for theophylline detection utilizing biorecognition elements such as enzymes

or nucleic acids, offering significant advantages in specificity and sensitivity.^{27–29} Biorecognition elements facilitate selective detection of theophylline, minimizing interference from other compounds and ensuring accurate quantification, even in complex biological samples.^{30–33} Their high sensitivity allows for detecting theophylline at low concentrations, making them particularly useful in medical and pharmaceutical applications. However, the utilization of biological parts in sensors comes with certain disadvantages such as the susceptibility to degrade over time, affecting their stability and operational lifespan.³⁴ Also, maintaining specific environmental conditions, such as optimal pH and temperature, is usually required to preserve their functionality, increasing the complexity and cost of their application.^{20,35}

As an alternative, electrochemical sensors without biorecognition elements have been explored for the detection of theophylline.^{1,9,20,36–46} These sensors depend on the direct oxidation of theophylline molecule offering advantages such as simplicity, cost-effectiveness, and long-term stability. They also provide excellent reproducibility, making them suitable for practical, real-world applications.²⁰ Numerous electrochemical sensors have been developed for theophylline detection using various platforms, including screen-printed electrodes, carbon fiber microdisk electrodes, gold electrodes, carbon paste electrodes, carbon nanotubes, and glassy carbon electrodes.^{1,9,36} These sensors have been applied in diverse mediums, such as human blood, urine, beverages like coffee, cola, black tea, green tea, fruit juices, and pharmaceutical formulations like drug tablets.^{1,9,20,36–46} There has been no report of electrochemical determination of theophylline in breast milk.

Most drugs taken by breastfeeding women transfer into breast milk posing potential short and long-term risks to the infant.⁴⁷ The transfer of medications into breast milk is a complex process involving multiple organ systems that play a role in drug metabolism, distribution, and excretion. Like many other drugs, theophylline is metabolized primarily in the liver before entering the systemic circulation.^{48,49} When the drug reaches the mammary glands through small capillaries, it can be transferred into breast milk via active transport, passive

diffusion, or apocrine secretion.⁵⁰ The extent of this transfer is measured by the milk-to-plasma ratio, which compares the drug concentration in breast milk to that in blood plasma. A higher ratio indicates increased drug secretion into milk, potentially leading to greater infant exposure.^{51–53}

Theophylline is one of the critical drugs that need to be monitored in breast milk due to its relatively high breast milk-to-plasma ratio (70%) and the potential side effects it may have on breastfed infants.^{54–56} Monitoring its levels in human milk can help protect infants from excessive exposure to theophylline. The quantification of theophylline in milk can help determine whether to continue with regular breastfeeding or implement the 'pump and dump' method, a practice in which breast milk is expressed to sustain supply, but is discarded rather than given to the infant, thus reducing the risk of harmful drug exposure. Also, quantifying theophylline in breast milk, combined with the known milk-to-plasma ratio, enables the estimation of its levels in maternal plasma. This approach provides a noninvasive and more accessible method for monitoring drug levels instead of taking and analyzing blood samples.

Despite the vital role of breast milk as a biofluid for diagnosis, nutrition assessment, and contamination detection, point-of-care technologies in this area remain largely unexplored.^{57,58} Remarkably, no sensor has yet been developed for theophylline detection, highlighting a critical gap in maternal and infant healthcare monitoring. In this study, we introduce the first rapid, accurate, portable, disposable, and cost-effective PoC device for the direct quantification of theophylline in breast milk, utilizing laser-induced graphene (LIG) electrodes. LIG was chosen for this application due to its unique combination of properties that make it ideal for electrochemical sensing. LIG offers a high surface area, excellent electrical conductivity, and chemical stability, which are crucial for achieving high sensitivity and accuracy in electrochemical analysis.^{59–61} Additionally, LIG electrodes are lightweight, easy to fabricate, and can be produced in a cost-effective and scalable manner, making them well-suited for portable, disposable sensor designs.^{62–67} Figure 1 summarizes theophylline's

medical uses, its presence in breast milk, its therapeutic range, and the development of a point-of-care (PoC) device for its quantification in breast milk.

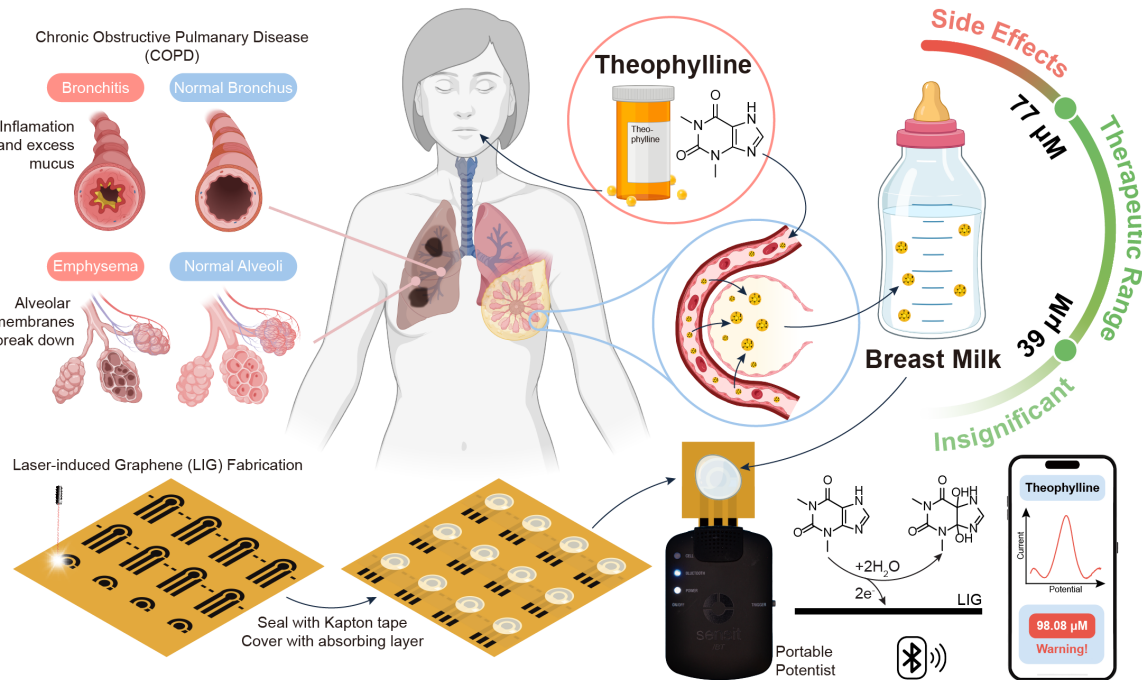


Figure 1: Theophylline’s medical applications, its transfer into breast milk, its therapeutic range, and the developed point-of-care (PoC) device for theophylline quantification in breast milk.

Results and discussion

Electrode Engraving and Material Characterization

The electrochemical PoC device was manufactured by engraving polyimide (PI) polymer sheets (127 μm in thickness) using a CO₂ laser (30 W) with a 9.3 μm wavelength to create laser-induced graphene (LIG) electrodes. This approach enables high scalability, reproducibility, and speed in producing high-quality graphitic structures without the need for additional physical or chemical treatments.^{62,68} LIGs exhibit outstanding electrical conductivity, remarkable flexibility, and strong electrochemical activity, making them highly suitable for various electrochemical applications, including medical diagnostics.^{63,65,69} LIG’s

electrochemical, structural, and mechanical properties are strongly influenced by the laser energy delivered per unit area of the substrate, which can be controlled by adjusting different factors such as laser power, spot size, and engraving speed. In our previous work, we optimized the engraving parameters to achieve the highest electrochemical conductivity and durable mechanical stability. The parameters obtained and used in this work include a laser power of 13%, an engraving speed of 20%, and a defocusing distance of 0.30 inches. These settings produce mechanically stable LIG with low sheet resistance ($7.2 \Omega/\text{sq}$) and maintain stable conductivity for up to 50 bending cycles.⁵⁸

Scanning Electron Microscopy (SEM) analysis was conducted to examine the surface morphology of the synthesized LIG. The top-view (Figure 2A&B) and cross-sectional SEM images of the LIG electrodes (Figure 2C) reveal the formation of a three-dimensional porous graphitic structure (the thickness is approximately $50 \mu\text{m}$). This highly porous architecture significantly increases the active surface area, enhancing the sensitivity of the electrochemical sensors. Also, the edge-plane sites on the LIG surface improve electron transfer efficiency on the electrode solution interface. Raman spectroscopy was employed to analyze the structural features of the synthesized LIG. As shown in the Raman spectrum (Figure 2D), three prominent peaks characteristic of a 3D graphitic structure are observed. The G peak, located around 1584 cm^{-1} , corresponds to the vibrational mode of sp^2 carbon atoms in the graphene framework. The D peak, appearing near 1348 cm^{-1} , signifies structural imperfections and defects within the graphene lattice of the LIG. Additionally, the 2D peak, observed at approximately 2706 cm^{-1} , reflects the presence of multilayered graphene. The $I_{2\text{D}}/I_{\text{G}}$ intensity ratio (0.63) further confirms the formation of a multilayered graphene structure.⁷⁰

The surface area of the LIG-based electrodes and the reproducibility of their fabrication process were assessed using cyclic voltammetry. Measurements were carried out within a potential window of -0.5 to 0.6 V versus an Ag/AgCl reference electrode, using an electrolyte solution containing $2.2 \text{ mM } [\text{Fe}(\text{CN})_6]^{3-/4-}$. As depicted in Figure 2E, the scan rates applied

were 30, 60, 90, 120, and 150 mV s⁻¹. A linear increase in the oxidation and reduction peak currents with the square root of the scan rates was observed, indicating a diffusion-controlled electrochemical process at the electrode surface, as shown in Figure 2F. The obtained current peaks were further analyzed using the Randles–Sevcik equation (Eq. 1):

$$i_p = 0.4463 nFAC \sqrt{\frac{nF\nu D}{RT}} \quad (1)$$

Here, i_p represents the peak current (A), n is the number of electrons transferred, F is the Faraday constant (C mol⁻¹), A is the electrode area (mm²), D is the diffusion coefficient (cm² s⁻¹), C is the electrolyte concentration (mol cm⁻³), ν is the scan rate (V s⁻¹), R is the gas constant (J K⁻¹ mol⁻¹), and T is the temperature (K). Using this equation, the active surface area of the LIG electrodes was calculated to be 60.83 ± 2.3 mm², which is almost 4.8 times higher than the geometric area (12.56 mm²). This improvement is ascribed to the highly porous structure of the LIG, which substantially increases the sensitivity of the LIG-based electroanalytical sensor.

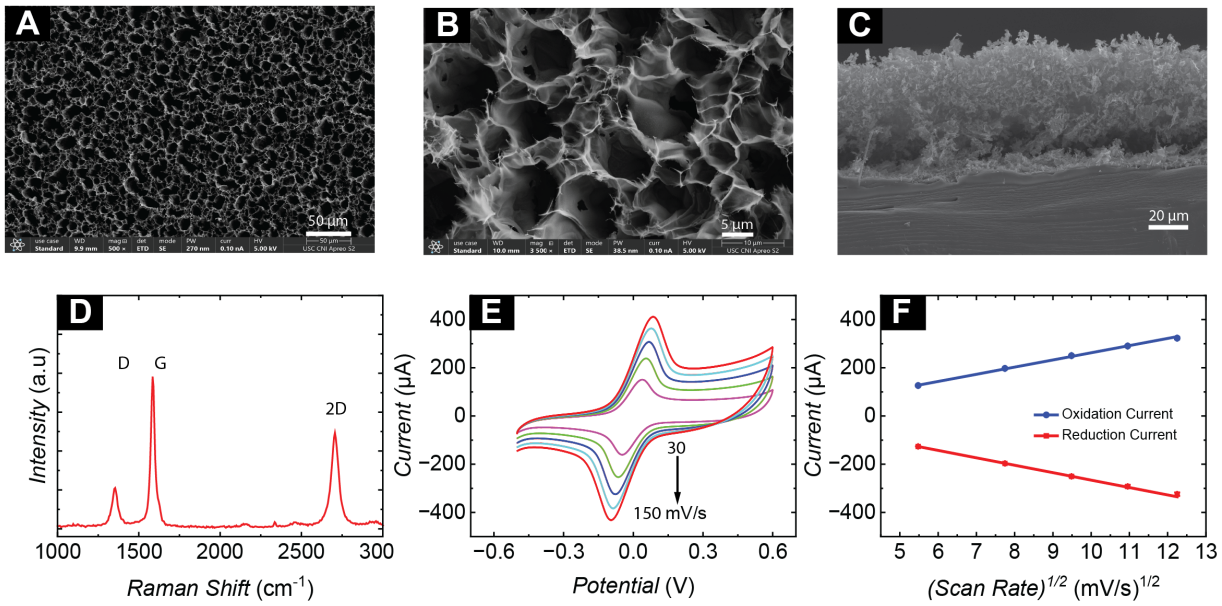


Figure 2: Characterization of LIGs. (A) and (B) are top SEM images for LIG at different scales. (C) Cross-sectional image of the Produced LIG material. (D) Raman spectrum of the LIG material. (E) Cyclic Voltammetry curves of the electrode obtained at scan rates of 30, 60, 90, 120 and 150 mV/s in 2.20 mM $[\text{Fe}(\text{CN})_6]^{3-/4-}$ in 0.1 M KCl as a supporting electrolyte. (F) Oxidation and reduction current peaks versus $(\text{scan rate})^{1/2}$ obtained from CVs in C, data represents mean \pm standard deviation (SD) for 4 electrodes.

Electrochemical Quantification of Theophylline in PBS

The developed LIGs were evaluated for their sensitivity toward theophylline. Figure 3A illustrates the mechanism of theophylline detection, which involves the transfer of two electrons and two protons during the oxidation process. The platform was utilized to detect theophylline within a concentration range of 0 to 150 μM in phosphate buffer saline (PBS) at pH 7.4. Square Wave Voltammetry (SWV) was employed for electroanalytical measurements and response recording over a potential range of 0.6 V to 1.1 V, with frequency, incremental step, and amplitude of 10 Hz, 4 mV, and 20 mV, respectively. SWV is a highly sensitive and versatile technique for electrochemical analysis due to its ability to enhance signal-to-noise ratios and precisely detect analytes at low concentrations. SWV voltammograms are shown in Figure 3B. The oxidation peak of theophylline was observed at a potential of

approximately 0.86 V, with the response increasing proportionally to the concentration of theophylline. Current peaks were used to construct the calibration curve, as shown in Figure 3D. The sensor demonstrated a linear response within the tested concentration range, with a calibration equation of (I (μ A) = 0.11 (μ M) + 1.99) and R^2 = 0.99.

The sensor demonstrated a limit of detection (LOD) of 4.7 μ M. The LOD was calculated using the formula $LOD = \frac{3.3\sigma}{s}$, where σ represents the standard deviation of three blank measurements, and s is the slope of the calibration curve in 3D. The sensor's wide dynamic range, high sensitivity, and low detection limit highlight its potential for future applications in complex matrices, such as breast milk, which offers robust and accurate detection of theophylline. The electrolyte solution's pH significantly influences theophylline's oxidation and its electrochemical properties. Changes in pH can affect the availability of protons within the solution, which in turn can alter the kinetics of the oxidation process of theophylline. To investigate this, we performed square wave voltammetry (SWV) measurements on 10 μ M theophylline in 0.1 M phosphate-buffered saline (PBS) at varying pH values ranging from 3.0 to 9.7. As depicted in Figure 3C, the oxidation potential of theophylline decreases with increasing pH, indicating that protons are involved in the electrochemical oxidation process. This trend suggests that the oxidation mechanism is influenced by the presence of protons in the solution, as higher pH values correspond to a reduction in the oxidation potential. The data further reveal a linear relationship between the solution's pH and theophylline's oxidation potential, with a slope of -61 mV/pH, as shown in Figure 3E. This slope is in close agreement with the theoretical Nernstian value of approximately -59 mV/pH, supporting the hypothesis that the oxidation of theophylline involves a coupled transfer of protons and electrons. The alignment of the experimental data with the Nernst equation suggests that the electrochemical oxidation of theophylline is a proton-electron process, where equal numbers of protons and electrons are involved, as illustrated in Figure 6A.

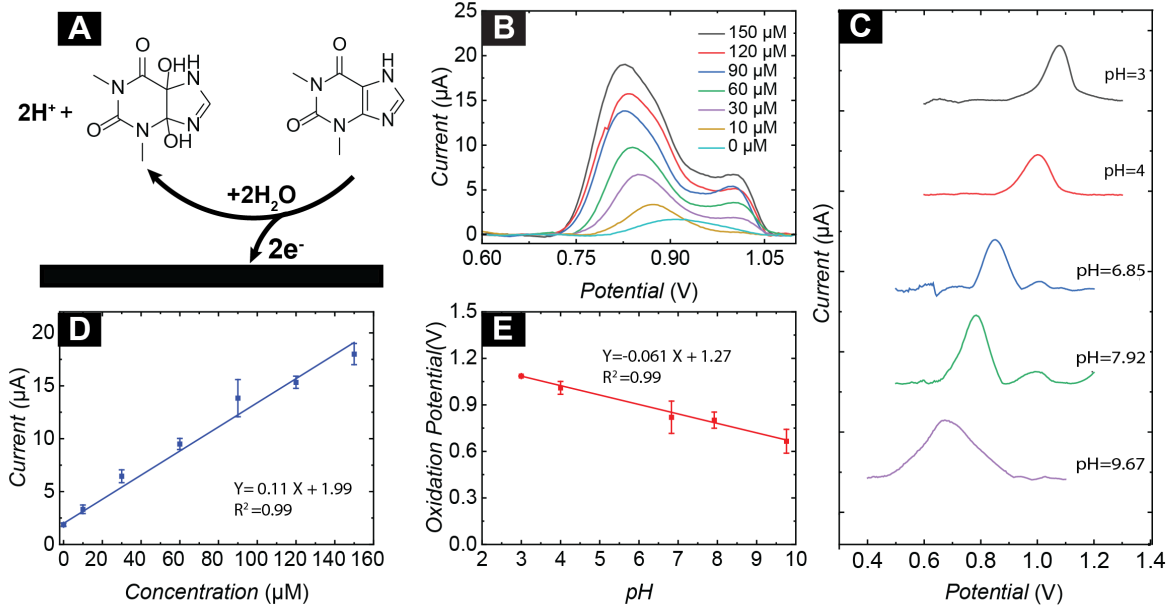


Figure 3: Characterization of theophylline oxidation in pH buffer. (A) Mechanism of theophylline oxidation on the LIG-based electrochemical electrode. (B) Square wave voltammograms with increasing theophylline concentration from 0 to 150 μM in PBS (pH=7.4). (C) SWVs of 10 μM theophylline at different pH values. (D) The calibration curve of LIG-based electrode response to theophylline concentrations in PBS (pH=7.4). (E) Correlation between SWV oxidation potential and pH value for theophylline. Error bars represent SD for 3 different electrodes.

Electrochemical Quantification of Theophylline in Human Milk

Following the successful detection of theophylline in PBS, we proceeded to evaluate the sensor's performance with non-diluted human milk samples spiked with theophylline. To facilitate the direct analysis of human milk in home settings, a glass fiber layer (0.25 cm^2) was placed on top of the sensing area of the electrode, functioning as an absorption layer for the milk samples. Frozen human milk samples were first thawed, sonicated at 37°C for 20 minutes, and then allowed to equilibrate to room temperature before measurements. A 70 μL aliquot of the milk sample was applied to the absorbing layer on the electrode surface, and measurements were performed immediately thereafter. To assess the suitability of the developed POC device for direct testing of milk samples without the need for further preparation, we initially employed linear sweep voltammetry (LSV) at a scan rate of 50

mV/s within a potential window of 0.6 to 1.3 V. As demonstrated in Figure 4A, the PoC device exhibited sensitivity to the oxidation of theophylline in human milk, with detectable concentrations ranging from 0 to 480 μ M. To obtain a calibration curve for theophylline in human milk, we used SWV for the calibration curve measurements. SWV provides a high resolution peak, more sensitivity and a lower detection limit.⁷¹

One common challenge in voltammetric measurements is the capacitive background current, which generates a baseline signal that can interfere with the accurate measurement of peak currents. To address this issue and improve the precision of peak height determination, a baseline correction procedure was applied. This was achieved through 3-order polynomial fitting, where the baseline is modeled by fitting a polynomial curve to the raw data, excluding the peak region. The true peak current is then obtained by subtracting this baseline from the raw voltammetric signal. To perform the baseline correction and other signal processing tasks, the Peakutils open-source Python library was employed. These tools offer reliable and efficient methods for analyzing scientific data. Figure 4B presents the raw SWV voltammogram obtained as a response to 60 μ M theophylline in human milk, along with the fitted baseline, while Figure 4C displays the processed data after subtracting the baseline from the raw SWV signal. This method was consistently applied to all measurements performed in human milk samples.

The sensor maintained a sensitive performance in the undiluted human milk as observed in Figure 4D. As shown in Figure 4E, the response exhibited a clear linear correlation with spiked theophylline concentrations ranging from 0 to 150 μ M in human milk. The calibration curve (Figure 4 D) demonstrated a sensitivity of 0.03 μ A/ μ M and a limit of detection (LOD) of 6.5 μ M. Importantly, the sensor effectively covered the physiological range of theophylline concentrations in breast milk (39 to 77 μ M) without requiring any sample preparation. To ensure the selectivity of our sensor for theophylline against naturally occurring substances in breast milk, we compared the sensor's response to 75 μ M theophylline in milk samples

collected at different lactation stages (1 month, 6 months, and 12 months postpartum). These samples typically exhibit varying compositions to meet the nutritional needs of the infants' growth phase. Specifically, fat, protein, and sugar content of breast milk change as the postpartum stage progresses to fulfill the energy and nutritional requirements of the baby.⁷²⁻⁷⁴ The results, shown in Figure 4F, indicate that these natural variations do not significantly affect the device's performance. This highlights the device's practicality in enabling simple, rapid, and direct point-of-care theophylline detection in human milk, supporting the health and well-being of both mothers and infants. Table 1 compares the analytical performance of the PoC theophylline device developed in this work with previously reported theophylline sensors in the literature.

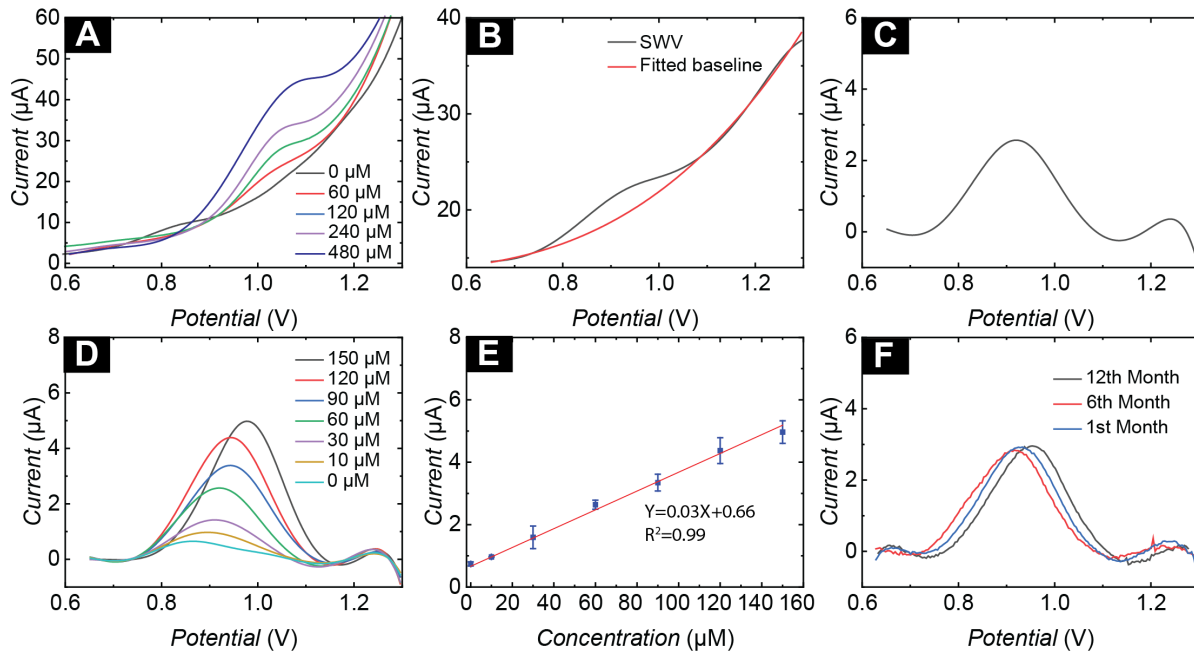


Figure 4: Electrochemical detection of theophylline in breast milk. (A) Linear sweep voltammograms (LSV) for different concentrations of theophylline in human milk. (B) The pristine square wave voltammograms (SWV) and fitted baseline obtained in response to 60 μM theophylline in human milk. (C) The response toward 60 μM theophylline in human milk after subtracting the baseline from the raw SWV signal. (D) SWVs with increasing theophylline concentration from 0 to 150 μM in human milk. (E) The calibration curve of the sensor response to theophylline concentrations in human milk. (F) SWV measurements for 75 μM theophylline in milk samples taken at the 1st, 6th, and 12th months postpartum. Error bars represent SD for 3 electrodes.

Table 1: Analytical performance of the PoC theophylline device (developed in this work) compared with theophylline sensors in the literature. The following abbreviations are used in the table. GCE: Glassy Carbon Electrode, g-C₃N₄: Glassy Carbon Electrode-modified graphitic carbon nitride, BDD: boron-doped diamond, SPE; Screen Printed Electrode, CPE: Carbon Paste Electrode, MB: Methylene Blue, DDAB: didodecyldimethylammonium bromide, ThOx: theophylline Oxidase

Electrode Surface	Detection Method	Sample	Linear Range μM	LOD μM	Reference
GCE/Graphene/Nafion MWCNT/CuO	DPV Potentiometric	Drug tablets Chinese black tea, Chinese green tea, Indian black tea, Indian green tea.	0.01 - 1, 2 - 30 0.1 - 10,000	0.006 0.025	⁷⁵ ⁷⁶
TiO ₂ NRs/MWCNT g-C ₃ N ₄ /GCE SPE/MB CPE/GO/CuO	DPV DPV DPV DPV	Urine, chocolate powder PBS Pharmaceutical and human urine samples Urine and pharmaceutical tablets	0.56-893 5.2 - 118μM 0.2 -10 0.02-209.6	0.56 0.043 0.002 0.01326	⁷⁷ ⁴³ ⁷⁸ ⁷⁹
SPCE/BDD/Au/DNA Aptamer AuSPE/DNA Aptamer	DPV SWV	Blood serum Blood samples Blood samples	1 to 100 2.75-225 0.2-50	0.0521 0.6 0.2	³³ ³² ³⁰
Graphite/Xanthine oxidase/ peroxidase/ferrocene Graphite/ThOx	Chronoamperometry Amperometric	Chronicamperometry Aqueous	200-2000	200	³¹
Graphite/ThOx/DDAB Laser-induced Graphene (LIG)	Chronoamperometry SWV	Aqueous Undiluted Human milk	20-600 0-150	20 6.5	⁸⁰ This work

Selectivity Studies

We evaluated the interference from other substances secreted into breast milk due to maternal intake such as alcohol and medications. These interferences included 20 mM alcohol, 200 μM paracetamol (a common painkiller), and several antibiotics typically administered postpartum to prevent infections. The antibiotics tested were ampicillin, cephalexin, cefotaxime, clindamycin, and gentamicin, each at a concentration of 200 μM. We used those concentrations to exceed their maximum expected physiological levels (Cmax) in breast milk to provide the highest interfering effect on the sensor performance. We compared the sensor response to 10 μM theophylline in human milk (6 months postpartum) with the response to the same concentration in the presence of one of these possible interferences in each experiment. As shown in Figure 5 A-H, all the tested potential interferences did not produce any noticeable effects or interfere with the detection of theophylline. Specifically, no additional peaks or signal disturbances were observed at the same electrochemical potential as theophylline, indicating that the sensor could selectively detect theophylline without interference from the tested substances. This selectivity is due to the distinct oxidation peak of theophylline, which occurs at a potential significantly different from that of potential interferents, minimizing

signal overlap. To ensure the robustness of the results, we repeated the experiments using three different sensors (Figure 5 I). This approach allowed us to verify the consistency of the sensor's performance and further assess whether the interfering substances influenced the measurement of theophylline. The results across all three sensors were consistent, with no detectable effect from the interfering molecules. This confirms the reliability of the sensor's selectivity and its potential for accurate, interference-free monitoring of theophylline levels in breast milk.

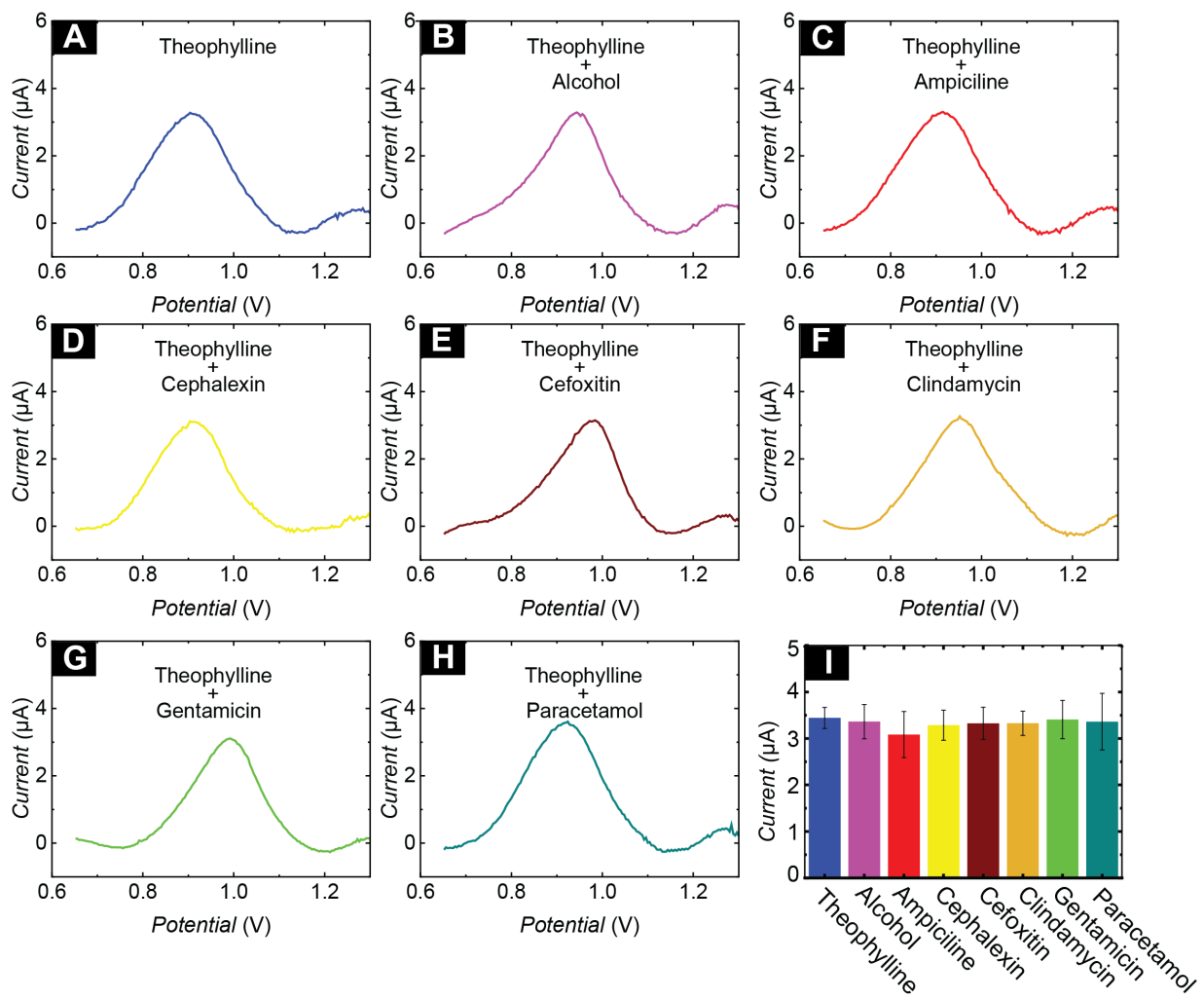


Figure 5: Selectivity studies. (A) Square wave voltammogram (SWV) showing the response to $10 \mu\text{M}$ theophylline in human milk. Interference study in human milk with $10 \mu\text{M}$ theophylline in the presence of: (B) 20 mM alcohol, (C) $200 \mu\text{M}$ ampicillin, (D) $200 \mu\text{M}$ cephalexin, (E) $200 \mu\text{M}$ paracetamol, (F) $200 \mu\text{M}$ clindamycin, (G) $200 \mu\text{M}$ cefotaxime, and (H) $200 \mu\text{M}$ gentamicin ($n=3$).

Recovery Measurements

After demonstrating the high sensitivity of the sensor to theophylline in both buffer and human milk, along with its excellent selectivity against naturally occurring variations in milk composition and potential interfering electroactive drugs, we proceeded to evaluate the accuracy of the sensor's measurements in real milk samples using the portable potentiostat. The goal was to assess the practical applicability and reliability of the method for home or point-of-care use, particularly for accurate theophylline quantification in milk, which is essential to ensure a safe lactating experience. To evaluate the accuracy of the measurements, we used a method in which theophylline concentrations in milk samples were adjusted to known levels of 20 μM , 75 μM , and 135 μM . These concentrations were prepared by dissolving theophylline directly into milk samples collected at 1 month, 6 months, and 12 months postpartum. The electrochemical measurements were conducted using a 70 μL sample size of the portable potentiostat, PalmSens, and analyzed using square wave voltammetry (SWV), as shown in Figure 6A. The results of the electrochemical measurements are shown in Figure 6B, C, & D for milk samples collected at the 1st, 6th, and 12th month postpartum, respectively, at theophylline levels of 0 μM , 20 μM , 75 μM , and 135 μM . The data in each figure clearly demonstrate an increase in current with increasing theophylline concentration, showing a strong and consistent correlation between the concentration of theophylline and the electrochemical response.

The recorded current from these measurements was used to quantify theophylline in the milk samples utilizing the generated calibration curve in Figure 4B. The accuracy of the measurements was calculated by comparing the measured concentrations of theophylline with the known concentrations for four different electrodes. The results of this comparison are summarized in Table 2, showing that the accuracy of the measurements ranged between 99.2% and 111%. These findings confirm the high reliability and accuracy of the sensor. The developed PoC device approach successfully demonstrates the ability to measure theophylline

levels in real human milk samples, with clear and reproducible electrochemical responses corresponding to known concentrations. The use of the portable potentiostat, PalmSens, enables easy, efficient, and rapid analysis of milk samples, which is crucial for ensuring proper management of theophylline therapy in lactating mothers.

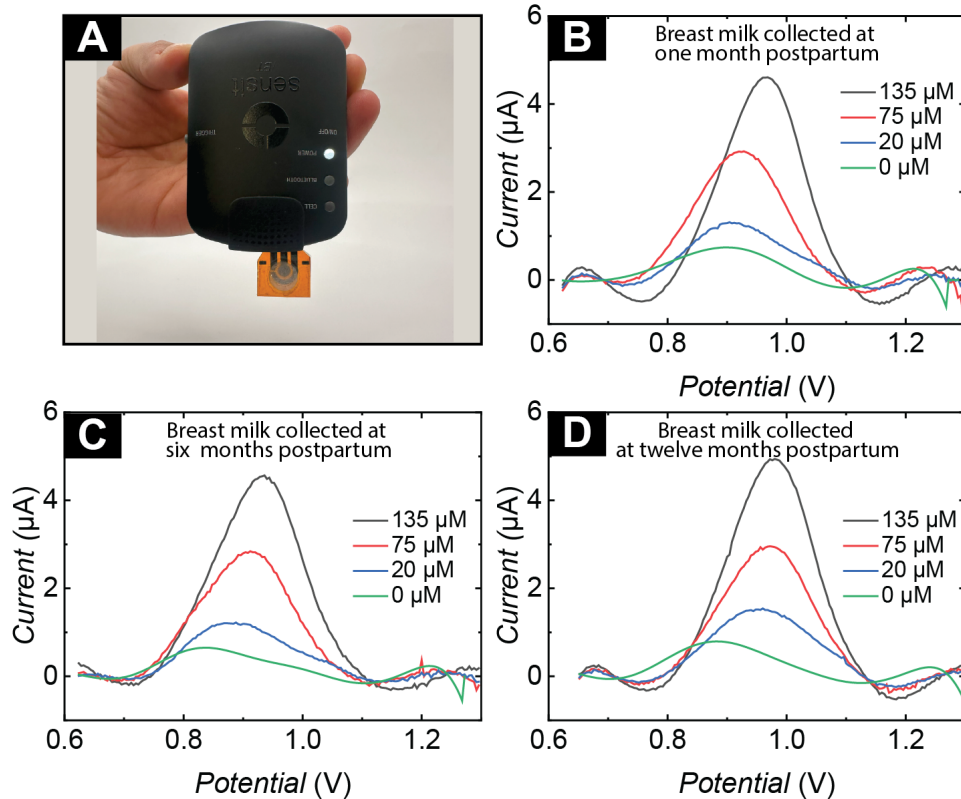


Figure 6: Recovery studies. (A) Image photo for the developed PoC device for theophylline detection. SWVs with increasing theophylline concentration from 0 to 135 μM in human milk taken at the (B) one, (C) six, and (D) 12 month postpartum.

Table 2: Detection accuracy of the developed PoC device for theophylline quantification in human milk samples taken at the 1st, 6th, and 12th months of lactation (n=4).

Sample	Spiked Concentration μM	Measured Concentration μM	Recovery %	RSD %
1st Month	20	22.0	110	12.7
	75	74.8	99.7	2.6
	135	137.4	101.8	4.5
6th Months	20	22.2	111	14.2
	75	75.4	100.5	5.2
	135	133.9	99.2	7.8
12th Months	20	21.3	106.5	12.3
	75	75.0	100.0	3.9
	135	138.6	102.7	6.0

Conclusion

Breastfeeding is crucial for both infant and maternal health, providing essential nutrients, immune support, and long-term protection against various diseases while also fostering mother-infant bonding. In addition to providing essential amino acids, nucleic acids, and immunological components necessary for a neonate's survival, breast milk can also contain biomarkers reflecting the mother's health, as well as contaminants such as drugs, inorganic pesticides, environmental pollutants, heavy metals, microplastics, antibiotics, and others. Therefore, analyzing breast milk offers critical insights into the mother's health, facilitating the identification of underlying medical conditions and enabling effective therapeutic monitoring. Also, this analysis is essential for ensuring that the infant receives nutritionally adequate milk, free from harmful contaminants promoting safe breastfeeding and optimal baby growth.

Theophylline is one of the medications that requires careful monitoring in breast milk. Although It is widely used in treating asthma and chronic obstructive pulmonary disease (COPD), theophylline has a narrow therapeutic range (55–110 μM in the blood), and at

overdose, it causes severe side effects such as nausea, arrhythmias, seizures, and even heart attack or death. Theophylline exhibits a high transfer ratio to breast milk, which (1) imposes high risks on breastfed infants, and (2) provides a valuable non-invasive way to estimate maternal serum levels by measuring its levels in human milk instead of blood samples. In this work, we used the electrochemical square wave voltammetry SWV technique for theophylline detection on a laser-induced graphene (LIG) electrode covered with an absorbing layer of fiberglass. The developed sensor successfully measures theophylline levels in breast milk directly in less than one minute through theophylline oxidation at the LIG surface, without requiring any sample preparation. The sensor demonstrates a sensitivity of $0.03 \mu\text{A}/\mu\text{M}$ and a limit of detection (LOD) of $6.5 \mu\text{M}$ in a range between 0 to $150 \mu\text{M}$, making it well-suited for monitoring theophylline concentrations in breast milk. Accurate measurements were achieved in spiked human milk samples collected at the one, six, and 12 months postpartum, with recovery rates ranging from 99.2% to 111.0%. This innovative point-of-care device represents a major advancement in maternal and infant healthcare by enabling mothers to monitor their medication levels and reduce the risk of neonatal exposure through breastfeeding.

Materials and Methods

Reagents and Solutions

We procured the following chemicals from Sigma-Aldrich (St. Louis, MO, USA): theophylline ($\text{C}_7\text{H}_8\text{N}_4\text{O}_2$), acetaminophen ($\text{CH}_3\text{CONHC}_6\text{H}_4\text{OH}$), potassium chloride (KCl), sodium hydroxide (NaOH), potassium ferricyanide ($\text{K}_3\text{Fe}(\text{CN})_6$), potassium ferrocyanide ($\text{K}_4\text{Fe}(\text{CN})_6$), cefoxitin, dicloxacillin, gentamicin, clindamycin, cephalexin, and ampicillin. We obtained electrical-grade Kapton® Polyimide Film ($12'' \times 12'' \times 0.005''$) from McMaster-Carr (USA) and Silver/silver chloride Ink (AGCL-1134) from Kayaku Advanced Materials (Westborough, MA, USA). Deionized water with a resistivity of $18.20 \text{ M}\Omega/\text{cm}$ was used to prepare the so-

lutions. Additionally, we sourced boric acid (99.5%), acetic acid (99.7%), and phosphoric acid (85.0%) from VWR (Radnor, PA, USA).

Electrode Fabrication

Laser-induced graphene (LIG) electrodes were fabricated on a polyimide (PI) film with a thickness of 127 μm . The film was sequentially cleaned with acetone, isopropyl alcohol, and deionized (DI) water, then dried at 90 °C for 10 minutes. The cleaned PI film was laser-engraved using a 30W CO₂ laser source operating at a wavelength of 9.3 μm (VLS 2.30, Universal Laser System Inc) in raster mode. Electrode patterns were created using Adobe Illustrator (Adobe, Inc.). The engraving was performed at a power of 13% and a speed of 20% of the maximum machine capability, with a defocusing distance of 0.3 inches above the laser focal point. After engraving, the electrodes were rinsed with DI water and thoroughly dried using nitrogen gas. Kapton tape was applied to define the surface area of the electrodes. The reference electrode was prepared by drop-casting Ag/AgCl ink onto the engraved reference area. The ink was dried at 90 °C for 30 minutes to ensure proper adhesion and functionality.

Material Characterization

We captured scanning electron microscopy (SEM) images using the FEI Nova NanoSEM 450 (FEI, OR, USA) and performed Raman spectroscopy with the Horiba XploRA Raman Microscope System (Horiba, Japan).

Electrochemical Measurements

For the electrochemical tests, square wave voltammetry (SWV) and cyclic voltammetry (CV) techniques were conducted using a CHI 760E potentiostat (CH Instruments, TX, USA). For wireless, on-site measurements on the theophylline point-of-care device, the Sensit BT device (PalmSens BV, Utrecht, Netherlands) was utilized. Electrochemical characterization

and determination of the electrode's active surface area were performed using CV in an electrolyte solution of 100 mM KCl and 2.2 mM $[\text{Fe}(\text{CN})_6]^{3-/4-}$, with a scan rate range between 30 and 150 mV⁻¹. We utilized a custom-printed circuit board (PCB) equipped with a Flat Flexible Cable (FFC) connector (FH34SRJ-18S-0.5SH(50)) to ensure a secure and straightforward connection between the LIG electrode and the benchtop potentiostat. Point-of-care measurements were performed using the Sensit BT potentiostat (PalmSens BV, Utrecht, Netherlands).

Milk Samples

All human sample-related experiments were approved by the Institutional Review Board at the University of Southern California (HS-23-00356), and the study adhered to the appropriate ethical guidelines and regulations. The human breast milk samples were provided by Mothers' Milk, an FDA-registered third-party milk bank, accredited by the Human Milk Banking Association of North America (HMBANA), and licensed as a tissue bank in California. In line with OHRP regulation 45 CFR 46.104, informed consent was not required to preserve donor anonymity, as the samples were anonymized and lacked any identifying information that could link them to the donors.

Acknowledgment

M. Mousavi acknowledges support from the 3M Nontenured Faculty Award, the Women in Science and Engineering (WiSE) program at the University of Southern California, the Zumberge Coordination Research Award, and the NIH Director's New Innovator Award (DP2GM150018). A. Al-Shami, M. Banks, S. Khazaee Nejad, A. Soleimani, H. Ma, F. Amirghasemi express their appreciation to the University of Southern California for the Viterbi Graduate Fellowship. The authors extend their sincere gratitude to Cu Ho, Nhat Nguyen, and the entire team at Mother's Milk for their invaluable collaboration in providing

samples and their dedication to advancing maternal and child health. Lastly, special thanks go to Dr. Christina Chambers and the team at the University of California San Diego Human Milk Institute for their support and contributions to this research.

Statistical Analysis

The data in this study are expressed as the mean \pm standard deviation, generally calculated for three independent measurements unless otherwise noted. Mean values, standard deviations, and linear regression analyses were calculated using Microsoft Excel.

References

- (1) Crapnell, R. D.; Banks, C. E. Electroanalytical overview: The electroanalytical detection of theophylline. *Talanta Open* **2021**, *3*, 100037.
- (2) Cui, Q.; Bian, R.; Xu, F.; Li, Q.; Wang, W.; Bian, Q. New molecular entities and structure–activity relationships of drugs designed by the natural product derivatization method from 2010 to 2018. *Studies in Natural Products Chemistry* **2021**, *69*, 371–415.
- (3) Ghosh, S.; Nandi, S.; Bhattacharjee, S. THERAPEUTIC EFFECTS & NEW PERSPECTIVE OF AN OLD DRUG THEOPHYLLINE. *American Journal of Pharmaceutical Research* **2024**, *14*.
- (4) Roche, N. Systemic medications in chronic obstructive pulmonary disease: Use and outcomes. *Clinics in Chest Medicine* **2020**, *41*, 485–494.
- (5) Barnes, P. J. *Epigenetics in Human Disease*; Elsevier, 2012; pp 387–393.
- (6) Marwick, J. A.; Caramori, G.; Stevenson, C. S.; Casolari, P.; Jazrawi, E.; Barnes, P. J.; Ito, K.; Adcock, I. M.; Kirkham, P. A.; Papi, A. Inhibition of PI3K δ restores glucocor-

- ticoid function in smoking-induced airway inflammation in mice. *American journal of respiratory and critical care medicine* **2009**, *179*, 542–548.
- (7) Karunarathna, I.; Gunawardana, K.; De Alvis, K.; Warnakulasooriya, A.; Fernando, C.; Rajapaksha, S.; others Aminophylline: A Comprehensive Review of its Therapeutic Window and Side Effects. *UVA Clinical Pharmacology* **2024**, *2*, 1–6.
- (8) Lee, K. S.; Kim, T.-H.; Shin, M.-C.; Lee, W.-Y.; Park, J.-K. Disposable liposome immunosensor for theophylline combining an immunochromatographic membrane and a thick-film electrode. *Analytica chimica acta* **1999**, *380*, 17–26.
- (9) Wang, T.; Randviir, E. P.; Banks, C. E. Detection of theophylline utilising portable electrochemical sensors. *Analyst* **2014**, *139*, 2000–2003.
- (10) Greene, S. C.; Halmer, T.; Carey, J. M.; Rissmiller, B. J.; Musick, M. A. Theophylline toxicity: An old poisoning for a new generation of physicians. *Turkish journal of emergency medicine* **2018**, *18*, 37–39.
- (11) Kilele, J. C.; Chokkareddy, R.; Rono, N.; Redhi, G. G. A novel electrochemical sensor for selective determination of theophylline in pharmaceutical formulations. *Journal of the Taiwan Institute of Chemical Engineers* **2020**, *111*, 228–238.
- (12) Barnes, P. J. Theophylline. *Pharmaceuticals* **2010**, *3*, 725–747.
- (13) Okada, A.; Sera, S.; Taguchi, M.; Yamada, H.; Nagai, N. Current status and usefulness of therapeutic drug monitoring implementation of theophylline in elderly patients based on a nationwide database study and modeling approach. *Science Progress* **2024**, *107*, 00368504241285122.
- (14) Krohmer, E.; Haefeli, W. E. Comment on: Increased Theophylline Plasma Concentrations in a Patient With COVID-19. *Annals of Pharmacotherapy* **2024**, 10600280241278336.

- (15) Srdjenovic, B.; Djordjevic-Milic, V.; Grujic, N.; Injac, R.; Lepojevic, Z. Simultaneous HPLC determination of caffeine, theobromine, and theophylline in food, drinks, and herbal products. *Journal of chromatographic science* **2008**, *46*, 144–149.
- (16) Zhang, Z.-Y.; Fasco, M. J.; Kaminsky, L. S. Determination of theophylline and its metabolites in rat liver microsomes and human urine by capillary electrophoresis. *Journal of Chromatography B: Biomedical Sciences and Applications* **1995**, *665*, 201–208.
- (17) El-Sayed, Y.; Islam, S. Comparison of fluorescence polarization immunoassay and HPLC for the determination of theophylline in serum. *Journal of Clinical Pharmacy and Therapeutics* **1989**, *14*, 127–134.
- (18) Cook, C.; Twine, M.; Myers, M.; Amerson, E.; Kepler, J.; Taylor, G. Theophylline radioimmunoassay: synthesis of antigen and characterization of antiserum. *Research communications in chemical pathology and pharmacology* **1976**, *13*, 497–505.
- (19) Linhares, M. C.; Kissinger, P. T. Pharmacokinetic studies using micellar electrokinetic capillary chromatography with in vivo capillary ultrafiltration probes. *Journal of Chromatography B: Biomedical Sciences and Applications* **1993**, *615*, 327–333.
- (20) Sutanto, L. G.; Sabilla, S.; Wardhana, B. Y.; Ramadani, A.; Sari, A. P.; Anjani, Q. K.; Basirun, W. J.; Amrillah, T.; Amalina, I.; Jiwanti, P. K. Carbon nanomaterials as electrochemical sensors for theophylline: a review. *RSC advances* **2024**, *14*, 28927–28942.
- (21) Al-Shami, A.; Oweis, R. J.; Al-Fandi, M. G. Developing an electrochemical immunosensor for early diagnosis of hepatocellular carcinoma. *Sensor Review* **2021**, *41*, 125–134.
- (22) Liu, X.; Wang, X.; Li, J.; Qu, M.; Kang, M.; Zhang, C. Nonmodified laser-induced graphene sensors for lead-ion detection. *ACS Applied Nano Materials* **2023**, *6*, 3599–3607.

- (23) Amirghasemi, F.; Nejad, S. K.; Chen, R.; Soleimani, A.; Ong, V.; Shroff, N.; Eftekhari, T.; Ushijima, K.; Ainla, A.; Siegel, S.; others LiFT (a Lithium Fiber-Based Test): An At-Home Companion Diagnostics for a Safer Lithium Therapy in Bipolar Disorder. *Advanced Healthcare Materials* **2024**, *13*, 2304122.
- (24) Ong, V.; Cortez, N. R.; Xu, Z.; Amirghasemi, F.; Abd El-Rahman, M. K.; Mousavi, M. P. An accessible yarn-based sensor for in-field detection of succinylcholine poisoning. *Chemosensors* **2023**, *11*, 175.
- (25) Makableh, Y. F.; Al-Fandi, M.; Jaradat, H.; Al-Shami, A.; Rawashdeh, I.; Harahsha, T. Electrochemical characterization of nanosurface-modified screen-printed electrodes by using a source measure unit. *Bulletin of Materials Science* **2020**, *43*, 1–6.
- (26) Chen, R.; Amirghasemi, F.; Ma, H.; Ong, V.; Tran, A.; Mousavi, M. P. Toward personalized treatment of depression: an affordable citalopram test based on a solid-contact potentiometric electrode for at-home monitoring of the antidepressant dosage. *ACS sensors* **2023**, *8*, 3943–3951.
- (27) Ansari, A.; Siddique, M. U. M.; Nayak, A. K.; Askari, V. R.; Zairov, R. R.; Aminab-havi, T. M.; Hasnain, M. S. *Fundamentals of Biosensors in Healthcare*; Elsevier, 2025; pp 1–20.
- (28) Ferapontova, E. E.; Olsen, E. M.; Gothelf, K. V. An RNA aptamer-based electrochemical biosensor for detection of theophylline in serum. *Journal of the American Chemical Society* **2008**, *130*, 4256–4258.
- (29) Lee, K. S.; Lee, W.-Y.; Park, J.-K. Disposable thick-film liposome immunosensor for theophylline using immunochromatographic matrix. Proceedings of International Solid State Sensors and Actuators Conference (Transducers' 97). 1997; pp 195–198.
- (30) Stredansky, M.; Pizzariello, A.; Miertus, S.; Svorc, J. Selective and sensitive biosensor

- for theophylline based on xanthine oxidase electrode. *Analytical Biochemistry* **2000**, *285*, 225–229.
- (31) Christenson, A.; Dock, E.; Gorton, L.; Ruzgas, T. Direct heterogeneous electron transfer of theophylline oxidase. *Biosensors and Bioelectronics* **2004**, *20*, 176–183.
- (32) Nguyen, M.-D.; Prevot, G. T.; Fontaine, N.; Dauphin-Ducharme, P. Whole blood theophylline measurements using an electrochemical DNA aptamer-based biosensor. *ECS Sensors Plus* **2024**, *3*, 030601.
- (33) Hartati, Y. W.; Syafira, R. S.; Irkham, I.; Zakiyyah, S. N.; Gunlazuardi, J.; Kondo, T.; Anjani, Q. K.; Jiwanti, P. K. A BDD-Au/SPCE-based electrochemical DNA aptasensor for selective and sensitive detection of theophylline. *Diamond and Related Materials* **2024**, *150*, 111725.
- (34) Martinkova, P.; Kostelnik, A.; Valek, T.; Pohanka, M. In Main streams in the Construction of Biosensors and Their Applications. *International Journal of Electrochemical Science* **2017**, *12*, 7386–7403.
- (35) Shanbhag, M. M.; Manasa, G.; Mascarenhas, R. J.; Mondal, K.; Shetti, N. P. Fundamentals of bio-electrochemical sensing. *Chemical Engineering Journal Advances* **2023**, *16*, 100516.
- (36) MansouriMajd, S.; Teymourian, H.; Salimi, A.; Hallaj, R. Fabrication of electrochemical theophylline sensor based on manganese oxide nanoparticles/ionic liquid/chitosan nanocomposite modified glassy carbon electrode. *Electrochimica Acta* **2013**, *108*, 707–716.
- (37) Zhang, H.; Wu, S.; Xing, Z.; Wang, H.-B.; Liu, Y.-M. A highly sensitive electrochemical sensor for theophylline based on dopamine-melanin nanosphere (DMN)-gold nanoparticles (AuNPs)-modified electrode. *Applied Physics A* **2021**, *127*, 1–9.

- (38) Di Matteo, P.; Trani, A.; Bortolami, M.; Feroci, M.; Petrucci, R.; Curulli, A. Electrochemical Sensing platform based on carbon dots for the simultaneous determination of theophylline and caffeine in tea. *Sensors* **2023**, *23*, 7731.
- (39) Jiwanti, P. K.; Sari, A. P.; Wafiroh, S.; Hartati, Y. W.; Gunlazuardi, J.; Putri, Y. M.; Kondo, T.; Anjani, Q. K. An Electrochemical sensor of theophylline on a boron-doped diamond electrode modified with nickel nanoparticles. *Sensors* **2023**, *23*, 8597.
- (40) Ghanbari, M. H.; Norouzi, Z.; Etzold, B. J. Increasing sensitivity and selectivity for electrochemical sensing of uric acid and theophylline in real blood serum through multi-nanocomposites. *Microchemical Journal* **2023**, *191*, 108836.
- (41) Mari, E.; Duraisamy, M.; Eswaran, M.; Sellappan, S.; Won, K.; Chandra, P.; Tsai, P.-C.; Huang, P.-C.; Chen, Y.-H.; Lin, Y.-C.; others Highly electrochemically active Ti₃C₂Tx MXene/MWCNT nanocomposite for the simultaneous sensing of paracetamol, theophylline, and caffeine in human blood samples. *Microchimica Acta* **2024**, *191*, 212.
- (42) Vinoth, S.; Wang, S.-F. Lanthanum vanadate-based carbon nanocomposite as an electrochemical probe for amperometric detection of theophylline in real food samples. *Food Chemistry* **2023**, *427*, 136623.
- (43) Dhamodharan, A.; Perumal, K.; Gao, Y.; Pang, H. Sensitive Detection of Theophylline Using a Modified Glassy Carbon Electrode with g-C₃N₄. *Chemistry Africa* **2024**, 1–10.
- (44) Zhu, Y.; Zhang, Y.; Hao, X.; Xia, Q.; Zhang, S. Highly sensitive detection of theophylline by differential pulse voltammetry using zinc oxide nanoparticles and multi-walled carbon nanotubes-modified carbon paste electrode. *Chemical Papers* **2024**, *78*, 7719–7728.
- (45) Moulick, M.; Das, D.; Nag, S.; Pramanik, P.; Roy, R. B. Gadolinium oxide modified molecular imprinted polymer electrode for the electrochemical detection of theophylline in black tea. *Journal of Food Composition and Analysis* **2025**, *137*, 106994.

- (46) Thanh, N. M.; Nam, N. G.; Dung, N. N.; Thu, P. T. K.; Man, N. Q.; Binh, N. T.; Khieu, D. Q.; others Electrochemical determination of theophylline using a nickel ferrite/activated carbon-modified electrode. *Materials Research Express* **2024**, *11*, 055006.
- (47) Fríguls, B.; Joya, X.; García-Algar, O.; Pallás, C.; Vall, O.; Pichini, S. A comprehensive review of assay methods to determine drugs in breast milk and the safety of breastfeeding when taking drugs. *Analytical and bioanalytical chemistry* **2010**, *397*, 1157–1179.
- (48) Sarkar, M. A.; Hunt, C.; Guzelian, P. S.; Karnes, H. T. Characterization of human liver cytochromes P-450 involved in theophylline metabolism. *Drug metabolism and disposition* **1992**, *20*, 31–37.
- (49) Kurata, Y.; Muraki, S.; Kashihara, Y.; Hirota, T.; Araki, H.; Ieiri, I. Differences in theophylline clearance between patients with chronic hepatitis and those with liver cirrhosis. *Therapeutic drug monitoring* **2020**, *42*, 829–834.
- (50) Gong, C.; Bertagnolli, L. N.; Boulton, D. W.; Coppola, P. A literature review of drug transport mechanisms during lactation. *CPT: Pharmacometrics & Systems Pharmacology* **2024**, *13*, 1870–1880.
- (51) Beers, J. L.; Hebert, M. F.; Wang, J. Transporters and drug secretion into human breastmilk. *Expert Opinion on Drug Metabolism & Toxicology* **2025**,
- (52) Abduljalil, K.; Pansari, A.; Ning, J.; Jamei, M. Prediction of drug concentrations in milk during breastfeeding, integrating predictive algorithms within a physiologically-based pharmacokinetic model. *CPT: pharmacometrics & systems pharmacology* **2021**, *10*, 878–889.
- (53) Le Marois, M.; Doudka, N.; Tzavara, E.; Delaunay, L.; Quaranta, S.; Blin, O.; Belzeaux, R.; Guilhaumou, R. Simultaneous quantification of psychotropic drugs in human plasma and breast milk and its application in therapeutic drug monitoring and peripartum treatment optimization. *Therapeutic Drug Monitoring* **2024**, *46*, 227–236.

- (54) Stec, G. P.; Greenberger, P.; Ruo, T. I.; Henthorn, T.; Morita, Y.; Atkinson Jr, A. J.; Patterson, R. Kinetics of theophylline transfer to breast milk. *Clinical Pharmacology & Therapeutics* **1980**, *28*, 404–408.
- (55) Purkiewicz, A.; Pietrzak-Fiećko, R.; Sörgel, F.; Kinzig, M. Caffeine, paraxanthine, theophylline, and theobromine content in human milk. *Nutrients* **2022**, *14*, 2196.
- (56) Abduljalil, K.; Gardner, I.; Jamei, M. Application of a physiologically based pharmacokinetic approach to predict theophylline pharmacokinetics using virtual non-pregnant, pregnant, fetal, breast-feeding, and neonatal populations. *Frontiers in Pediatrics* **2022**, *10*, 840710.
- (57) Ojara, F. W.; Kawuma, A. N.; Waitt, C. A systematic review on maternal-to-infant transfer of drugs through breast milk during the treatment of malaria, tuberculosis, and neglected tropical diseases. *PLoS Neglected Tropical Diseases* **2023**, *17*, e0011449.
- (58) Al-Shami, A.; Ma, H.; Banks, M.; Amirghasemi, F.; Mohamed, M. A.; Soleimani, A.; Khazaee Nejad, S.; Ong, V.; Tasso, A.; Berkmen, A.; others Mom and Baby Wellness with a Smart Lactation Pad: A Wearable Sensor-Embedded Lactation Pad for on-Body Quantification of Glucose in Breast Milk. *Advanced Functional Materials* **2025**, 2420973.
- (59) Marques, A. C.; Cardoso, A. R.; Martins, R.; Sales, M. G. F.; Fortunato, E. Laser-induced graphene-based platforms for dual biorecognition of molecules. *ACS Applied Nano Materials* **2020**, *3*, 2795–2803.
- (60) Park, H.; Kim, M.; Kim, B. G.; Kim, Y. H. Electronic functionality encoded laser-induced graphene for paper electronics. *ACS Applied Nano Materials* **2020**, *3*, 6899–6904.
- (61) Griesche, C.; Hoecherl, K.; Baeumner, A. J. Substrate-independent laser-induced

- graphene electrodes for microfluidic electroanalytical systems. *ACS Applied Nano Materials* **2021**, *4*, 3114–3121.
- (62) Al-Shami, A.; Amirghasemi, F.; Soleimani, A.; Khazaee Nejad, S.; Ong, V.; Berkmen, A.; Ainla, A.; Mousavi, M. P. SPOOC (Sensor for Periodic Observation of Choline): An Integrated Lab-on-a-Spoon Platform for At-Home Quantification of Choline in Infant Formula. *Small* **2024**, 2311745.
- (63) Soleimani, A.; Amirghasemi, F.; Al-Shami, A.; Nejad, S. K.; Tsung, A.; Wang, Y.; Galindo, S. L.; Parvin, D.; Olson, A.; Avishai, A.; others Towards sustainable and humane dairy farming: A low-cost electrochemical sensor for on-site diagnosis of milk fever. *Biosensors and Bioelectronics* **2024**, 259, 116321.
- (64) Ma, H.; Nejad, S. K.; Ramos, D. V.; Al-Shami, A.; Soleimani, A.; Amirghasemi, F.; Mohamed, M. A.; Mousavi, M. P. Lab-on-a-lollipop (LoL) platform for preventing food-induced toxicity: all-in-one system for saliva sampling and electrochemical detection of vanillin. *Lab on a Chip* **2024**, *24*, 4306–4320.
- (65) Amirghasemi, F.; Al-Shami, A.; Ushijima, K.; Mousavi, M. P. Flexible Acetylcholine Neural Probe with a Hydrophobic Laser-Induced Graphene Electrode and a Fluorous-Phase Sensing Membrane. *ACS Materials Letters* **2024**, *6*, 4158–4167.
- (66) Nejad, S. K.; Ma, H.; Al-Shami, A.; Soleimani, A.; Mohamed, M. A.; Dankwah, P.; Lee, H. J.; Mousavi, M. P. Sustainable agriculture with LEAFS: a low-cost electrochemical analyzer of foliage stress. *Sensors & Diagnostics* **2024**, *3*, 400–411.
- (67) Li, Z.; Huang, L.; Cheng, L.; Guo, W.; Ye, R. Laser-Induced Graphene-Based Sensors in Health Monitoring: Progress, Sensing Mechanisms, and Applications. *Small Methods* **2024**, 2400118.
- (68) Lin, J.; Peng, Z.; Liu, Y.; Ruiz-Zepeda, F.; Ye, R.; Samuel, E. L.; Yacaman, M. J.;

- Yakobson, B. I.; Tour, J. M. Laser-induced porous graphene films from commercial polymers. *Nature communications* **2014**, *5*, 5714.
- (69) Torrente-Rodríguez, R. M.; Lukas, H.; Tu, J.; Min, J.; Yang, Y.; Xu, C.; Rossiter, H. B.; Gao, W. SARS-CoV-2 RapidPlex: a graphene-based multiplexed telemedicine platform for rapid and low-cost COVID-19 diagnosis and monitoring. *Matter* **2020**, *3*, 1981–1998.
- (70) Bleu, Y.; Bourquard, F.; Loir, A.-S.; Barnier, V.; Garrelie, F.; Donnet, C. Raman study of the substrate influence on graphene synthesis using a solid carbon source via rapid thermal annealing. *Journal of Raman Spectroscopy* **2019**, *50*, 1630–1641.
- (71) Alyamni, N.; Abot, J. L.; Zestos, A. G. Perspective—advances in voltammetric methods for the measurement of biomolecules. *ECS sensors plus* **2024**, *3*, 027001.
- (72) Filatava, E. J.; Shelly, C. E.; Overton, N. E.; Gregas, M.; Glynn, R.; Gregory, K. E. Human milk pH is associated with fortification, postpartum day, and maternal dietary intake in preterm mother-infant dyads. *Journal of Perinatology* **2023**, *43*, 60–67.
- (73) Ford, E. L.; Underwood, M. A.; German, J. B. Helping mom help baby: nutrition-based support for the mother-infant dyad during lactation. *Frontiers in nutrition* **2020**, *7*, 54.
- (74) Innis, S. M. Impact of maternal diet on human milk composition and neurological development of infants. *The American journal of clinical nutrition* **2014**, *99*, 734S–741S.
- (75) Li, Y.; Wu, S.; Luo, P.; Liu, J.; Song, G.; Zhang, K.; Ye, B. Electrochemical behavior and voltammetric determination of theophylline at a glassy carbon electrode modified with graphene/nafion. *Analytical Sciences* **2012**, *28*, 497–502.
- (76) Al-Haidari, R. A.; Abdallah, N. A.; Al-Oqail, M. M.; Al-Sheddi, E. S.; Al-Massarani, S. M.; Farshori, N. N. Nanoparticles based solid contact potentiometric

sensor for the determination of theophylline in different types of tea extract. *Inorganic Chemistry Communications* **2020**, *119*, 108080.

- (77) Patel, B. R.; Imran, S.; Ye, W.; Weng, H.; Noroozifar, M.; Kerman, K. Simultaneous voltammetric detection of six biomolecules using a nanocomposite of titanium dioxide nanorods with multi-walled carbon nanotubes. *Electrochimica Acta* **2020**, *362*, 137094.
- (78) Bukkitgar, S. D.; Shetti, N. P. Electrochemical behavior of theophylline at methylene blue dye modified electrode and its analytical application. *Materials Today: Proceedings* **2018**, *5*, 21474–21481.
- (79) Patil, V. B.; Malode, S. J.; Mangasuli, S. N.; Tuwar, S. M.; Mondal, K.; Shetti, N. P. An electrochemical electrode to detect theophylline based on copper oxide nanoparticles composited with graphene oxide. *Micromachines* **2022**, *13*, 1166.
- (80) Ferapontova, E. E.; Shipovskov, S.; Gorton, L. Bioelectrocatalytic detection of theophylline at theophylline oxidase electrodes. *Biosensors and Bioelectronics* **2007**, *22*, 2508–2515.